BIORESEARCH OPEN ACCESS
Volume 1, Number 1, 2012

DOI: 10.1089/biores.2012.0211

Permeability of Three-Dimensional Fibrin Constructs Corresponds to Fibrinogen and Thrombin Concentrations

Cecilia L. Chiu, Vivian Hecht, Haison Duong, Benjamin Wu, and Bill Tawil

Abstract

Research in the last few years have focused on the use of three-dimensional (3D) fibrin construct to deliver growth factors and cells. Three-dimensional construct permeability and porosity are important aspects for proper nutrient uptake, gas exchange, and waste removal—factors that are critical for cell growth and survival. We have previously reported that the mechanical strength (stiffness) of 3D fibrin constructs is dependent on the fibrinogen and thrombin concentration. In this study, we established two new *in vitro* models to examine how fibrin composition affects the final 3D fibrin construct permeability and pore size; thereby, influencing the diffusivity of macromolecules throughout the network of fibrin fibrils. Flow measurements of both liquid and fluoresceinated-dextran microparticles are conducted to calculate the permeability and pore size of 3D fibrin constructs of different fibrinogen and thrombin concentrations. Similarly, the diffusivity of liquid and fluoresceinated-dextran microparticles through these 3D fibrin constructs are determined through diffusion models. Data from these studies show that the structural permeability and pore size of 3D fibrin constructs directly correlate to fibrinogen and thrombin concentration in the final 3D fibrin construct. More specifically, at a constant thrombin concentration of 2 or 5 μ/mL, pore size of the 3D fibrin constructs is dependent on fibrinogen if the concentration is 5 mg/mL and to a lesser extent if the concentration is 10–15 mg/mL. These findings suggest that fibrin's diffusive property can be manipulated to fabricate 3D constructs that are optimized for cellular growth, protein transport, and for the controlled delivery of bioactive molecules such as growth factors.

Key words: diffusivity; fibrin; fibrinogen; permeability; pore size

Introduction

Fibrin has been used extensively as a biomaterial for various tissue engineering and clinical applications.[1–6] Its structural, biochemical, and mechanical properties have been studied at length.[7–10] Fibrin is made from two main components: fibrinogen and thrombin. In the presence of Ca^{2+}, fibrinogen, a soluble 340-kDa clotting factor, is polymerized by the protease thrombin.[4,11,12] Factor XIIIa promotes cross-linkage between fibrinogen peptides to form a meshwork of fibrin fibrils.[13]

One aspect of studying biomaterials used in generating three-dimensional (3D) constructs is their permeability for nutrients and waste. Permeability of a 3D construct, regardless of the biomaterials used, depends on the pore size.[14,15] In the case of fibrin, pore size depends on the thickness and density of fibrin fibrils, which subsequently depend on fibrinogen and thrombin concentration.[16] The scaffold's porous structure, a combination of microporous (pore diameters <2 nm), mesoporous (pores with diameter 2–50 nm), or macroporous (pore diameters >50 nm) void spaces,[17] plays a major role in cellular penetration and tissue growth.[18,19] Interconnectivity refers to the extent of how much pores are connected with their neighboring pores, and has a large effect on nutrient and waste diffusion, cell migration, and overall scaffold permeability.[20] Thus, 3D construct permeability and porosity are of extreme importance to tissue engineering.

Fibrin-based materials have gained considerable interests in the field of tissue engineering in recent years.[4,5] For applications in cell culturing, it is vital for fibrin porosity to support sufficient nutrient uptake and cellular transport. While larger pores may allow for increased cell growth rates, fibrin scaffold integrity must not be compromised due to a weaker support from the decreased amount of cross-linking activity. The delicate balance between porosity and mechanical strength requires precision in tailoring the ideal 3D fibrin construct satisfying the needs of each cell line. In this article, two new *in vitro* models were established to analyze porosity in 3D fibrin constructs by changing fibrinogen and thrombin concentrations used for fabricating the 3D fibrin constructs.

Department of Bioengineering, University of California, Los Angeles, California.

Flow measurements were performed using a modified vertical column apparatus. This apparatus utilizes Darcy's law to calculate the average pore size in each 3D fibrin construct based on fluid flow rates through the fibrin construct. The second model consists of allowing Dextran particles to diffuse through the construct over time. Overall results show that increased fibrinogen concentrations cause a decrease in flow rates, diffusion rate, and consequently porosity.

Materials and Methods

Materials

Three-dimensional fibrin constructs were prepared using Fibrin Sealant Kits (Tisseel® Sealant Kit; Baxter Healthcare, Deerfield, IL) containing human fibrinogen, human thrombin, tris-glycine buffer, calcium chloride, and Aprotinin (fibrinolysis inhibitor). For flow and diffusion measurements, neutrally charged Fluoresceinyl isothiocyanato-dextran (FITC-dextran) (m.w. 3000 Da) and Rhodamine B-dextran (Rho-dextran) (m.w. 70,000) beads were purchased from Invitrogen (Carlsbad, CA).

Flow measurements using a modified in vitro *3D fibrin construct assay*

Preparation of 3D fibrin constructs in a modified flow measurement apparatus. Fibrinogen and thrombin solutions were prepared according to kit instructions (Fig. 1A). Briefly, fibrinogen (100 mg/mL) was reconstituted in 40 mM tris-glycine containing 3000 kIU/mL of aprotinin at 37°C. Thrombin (500 IU) was reconstituted in 40 mM of $CaCl_2$. Three-dimensional fibrin constructs were prepared by mixing various fibrinogen concentrations of 5–20 mg/mL (final concentration) with various thrombin concentrations of 2–20 IU/mL. Figure 1A illustrates a flow apparatus modified from a method described in He et al.[21] For our purpose, 3D fibrin constructs were prepared in modified Spin-X® centrifuge tube filter inserts (Fisher Scientific, Irvine, CA) where the nylon membrane was removed from the bottom of each insert, leaving a porous plastic base upon which the fibrin constructs were prepared. To prevent possible void space or fluid leakage between the fibrin matrix and the walls of the insert, the insert was coated (overnight and air-dried) with a fibrinogen solution that corresponded to the fibrin matrix formulation. For example, a 3D fibrin construct comprised 10 mg/mL of fibrinogen and 2 IU/mL of thrombin; the coating solution consisted of a 10 mg/mL fibrinogen solution. Three hundred microliters each of the prediluted fibrinogen and thrombin solutions was injected into the coated insert using a dual-barrel syringe (Discus Dental, Culver City, CA). The fibrin constructs were allowed to polymerize for 2 h at room temperature. The final dimensions of the 3D fibrin construct inside each insert were on average 12.25 mm in height, with a radius of 4 mm, yielding a total surface area of 408 mm^2. To check for leaks, the construct-containing inserts were eluted with 10 mL of phosphate-buffered saline dyed with food coloring. The inserts were blotted onto paper towel and the dye-diffusion impression was visualized. A dye impression of a clean and circular patch was indicative of a good seal. Those that had smudges around the edges of the impression were considered leaky and discarded. Subsequently, each matrix-containing insert was attached to a reservoir constructed from a 60-mL syringe that was trimmed at the tip to tightly connect the insert to form a seamless column. The insert–reservoir connection was sealed with silicon glue to prevent leakage. The entire elution column containing the reservoir–matrix-insert was attached to a vertical stand where a small receiving vial was placed to catch solution from the matrix-insert.

Flow through 3D fibrin constructs. Serum-free Dulbecco's modified Eagle's medium (DMEM) was used as the elution fluid. Before making measurements, the 3D fibrin constructs were equilibrated with the elution buffer to allow the fluid to fill the pores and achieve laminar flow. Flow measurements were made at different hydrostatic pressure heads (p-heads) to determine reproducibility of measurements. The hydrostatic pressure head was determined by the height of the elution medium in the 60-mL syringe reservoir, which included the area above the surface of the 3D fibrin construct. Depending on the volume of the reservoir, various heights of 3–12 cm yielding different p-heads were achieved by various elution volumes to the 60-mL syringe reservoir. At each p-head, the elution medium was allowed to flow through the 3D fibrin construct for 1 h. For each hourly time point, the eluate was collected and the height of the liquid remaining in the syringe reservoir was recorded. For the next hourly time point, the liquid level in the syringe reservoir was filled to the same level that was designated for that particular p-head. This was done for every subsequent time points. A total of six effluent volumes were collected over six hourly periods for each 3D fibrin construct tested. The 3D fibrin construct permeability and average pore size were calculated using Darcy's law. Darcy's law is used to analyze fluid dynamics in a porous medium by evaluation of the Darcy coefficient of permeability (K_s). Equations for K_s and pore radii calculations are adapted from Okada and Blombäck.[22] The value of K_s can be determined by Equation 1:

$$K_s = \frac{Q}{t} \times \frac{L \times \eta}{A \times \Delta P} \quad (1)$$

where Q/t is the flow rate (cm^3/s), L is the height of the column measured from the surface of liquid to the bottom of the fibrin (cm), η is the viscosity of the media (poise), A is the surface area of the fibrin and liquid interface (cm^2), and P is the hydrostatic pressure (poise). The hydrostatic pressure is measured from the top of the media level that rested above the 3D fibrin construct. Flow rate was measured by the amount of percolating liquid that was eluted from the 3D fibrin construct. By calculating K_s, the average pore size of the fibrin matrix was estimated through the relationship between the permeability coefficient and radius of each pore distributed over the fibrin network. Using the estimated K_s values obtained from the flow measurements, the average radius r of the pores in each 3D fibrin construct was estimated by Equation 2:

$$r = \sqrt{8K_s/\varepsilon} \quad (2)$$

where ε is fractional void volume of the gel and r is measured in cm.

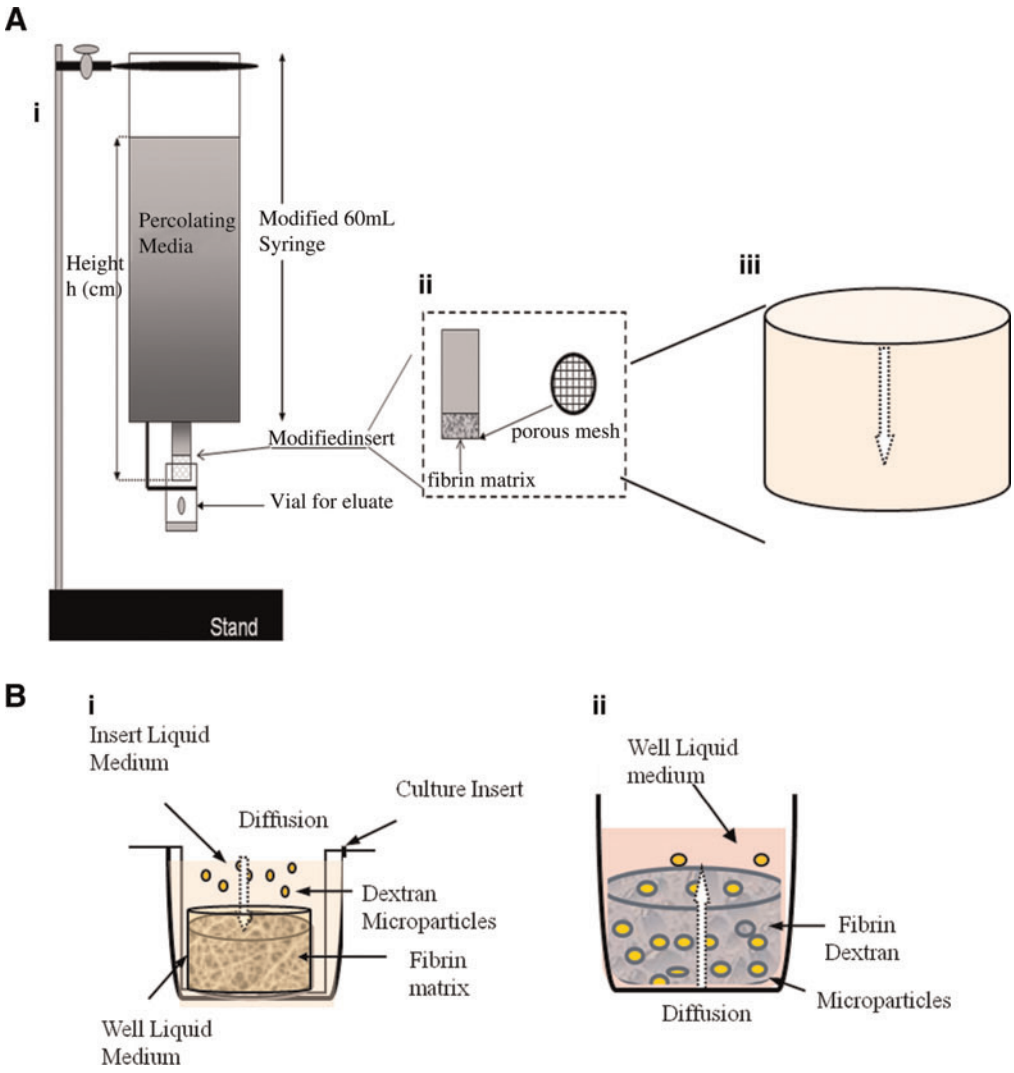

FIG. 1. New *in vitro* flow and diffusion assays. **(A)** Modified flow apparatus. Fibrin samples were made with 8–20 mg/mL fibrinogen concentration solutions mixed with a constant thrombin concentration solution at 2 IU/mL. **(i)** The apparatus was made using a 60-mL syringe as the reservoir for the permeation liquid, being serum-free DMEM. **(ii)** An insert containing the fibrin construct of varying fibrinogen concentration was attached via silicon glue to make a leak-proof seal. This insert was made from using modified Spin-X centrifuge tube filter inserts, where the membrane was removed from the inner base of the original insert. **(iii)** Fibrin constructs were prepared on mesh at the bottom of the inserts allowing eluate to come through with minimal obstruction. The eluate consisted of serum-free DMEM ± FITC-dextran or Rhodamine-Dextran microparticles. The eluates were collected at various hydrostatic pressures. **(B)** Modified diffusion apparatus. **(i)** Uptake-diffusion system: Diffusion assessment is performed over various fibrin scaffolds. At 24 h, 100-μL samples were taken from the top of the fibrin scaffold (nondiffused dextran) and from the bottom of each well (diffused dextran). Samples were transferred to a black plate reader for minimal light exposure. **(ii)** Release-diffusion system: Fibrin gels were formed in inserts fitted with 8.0-μm membrane. Serum-free DMEM was used as the media. Media level in the well rests at the same level to the bottom of the fibrin sample. The volume of the fibrin, media above the fibrin, and media in the well are 1, 0.5, and 1.5 mL, respectively. DMEM, Dulbecco's modified Eagle's medium; FITC, fluorescein isothiocyanate.

Flow measurements

Dextran flow through 3D fibrin construct. Fluorescein isothiocyanate (FITC; 3000 MW) and Rhodamine (RHO; 70,000 MW)-conjugated dextran particles, prepared at 10 and 25 μg/mL, respectively, were added to the top of the above column. Similar calculations to the liquid flow described above were made.

Diffusion measurements using a modified in vitro *3D fibrin construct assay*

Preparation of 3D fibrin constructs in a modified diffusion measurement apparatus. One-milliliter 3D fibrin constructs were formed in BD Falcon Cell Culture Inserts fitted with 8.0-μm pore size, high pore density (HD) translucent poly (ethylene terephthalate) membranes (catalog #353182;

Fisher). The inserts were placed in Falcon Multiwell, 12-well plates (catalog #353043; Fisher) (Fig. 1B). Each insert was first coated with the same coating method as described in the flow assessment (2.5, 5, 10, and 15 mg/mL fibrinogen solutions). The coating was allowed to polymerize overnight to ensure a good layer of coating fibrinogen to the inserts. Any excess coating fibrinogen was removed before overnight polymerization. An example of insert placement in the 12-well plates for each fibrin sample is shown in Figure 1B. Subsequently, 500 μL of the appropriate fibrinogen and thrombin solutions was placed in a dual-barrel syringe (Discus Dental) and quickly ejected into the appropriately coated inserts. The fibrin gels were allowed to polymerize in room temperature for 2 h, undisturbed. Each 3D fibrin construct measures at 10 mm in diameter and 5 mm in height with an average total surface area of 314 mm^2.

Dextran particles flow through 3D fibrin construct. In minimal lighting, 500 μL serum-free DMEM with fluorescein isothiocyanate (FITC; 3000 MW) and Rhodamine (RHO; 70,000 MW)-conjugated Dextran particles, prepared at 10 and 25 μg/mL, respectively, were added to the top of each scaffold. About 1.5 mL of serum-free DMEM was then added to the well holding each insert. Each plate was covered with aluminum foil and kept at room temperature. At 24 h after diffusion, 100-μL samples were taken from the top of the 3D fibrin construct as well as the bottom of the well for quantitative analysis of Dextran particles. Each sample was placed in a black plate reader to prevent light from reaching Dextran particles. Fluorescence of Dextran particles were measured on an Infinite 200 series microplate reader (Tecan, San Jose, CA).

Statistical analysis

Statistical analysis was performed using *t*-tests for both Darcy flow and Dextran diffusion assessments. Darcy flow assessment was performed in quadruplicates, whereas the Dextran diffusion assessment was performed in triplicates. Dextran standard curves for Rho and FITC were made through linear regression analysis. Graphs, tables, and statistical functions were made through GraphPad Prism® 4 analysis software (GraphPad Software Inc, San Diego, CA).

Results

Two new in vitro *methods to measure flow and diffusion in a 3D fibrin construct*

To study flow and diffusion through a 3D fibrin construct, we have established two new *in vitro* models. The first model (Fig. 1A) is a flow apparatus to study the rate of liquid transport through the 3D fibrin network of varying compositions. This model is relevant to the type of transport as observed in the intercapillary systems found *in vivo*.

The second model (Fig. 1B, i) is designed to study the uptake diffusion of FITC and RHO-Dextran particles through the fibrin network. This is relevant to the uptake of nutrients and transport of molecules necessary for cell survival within the 3D fibrin construct. A modification of the same model (Fig. 1B, ii) is designed to study the release diffusion of FITC and RHO-Dextran particles from a 3D fibrin construct. This system shows monolithic diffusion or release of molecules from the network of a 3D fibrin construct. This is relevant to potential use of 3D fibrin construct as delivery vehicles for growth factors or to study the retention and release efficiency of molecules by the network of the 3D fibrin construct. We have not presented the results from the release diffusion assay in this article.

Flow study in a 3D fibrin construct–effect of fibrinogen and thrombin concentration

We examined the effect of fibrinogen and thrombin composition on liquid mass transport through a 3D fibrin construct as facilitated by various hydrostatic pressures. Results showed that there is a decrease trend in the total volume of liquid eluted corresponding to increase in the fibrinogen component from 5 to 15 mg/mL at thrombin concentrations (2–20 IU/mL; Fig. 2A), except at the fibrinogen concentration of 15 mg/mL, where both 10 and 20 IU/mL showed no difference. However, as the thrombin concentration was increased from 2 to 20 IU/mL, the total eluted volume was the same for the three fibrinogen concentrations tested (5, 10, and 15 mg/mL) except at the thrombin concentration 2 IU/mL, where the increase in fibrinogen concentration showed a decrease in the eluted liquid. This may suggested that under the hydrostatic pressure the flow of liquid should be equal for all fibrin 3D constructs of similar porosity; however, the different composition of the fibrinogen and thrombin components may alter the porosity of the matrices, thereby affecting the movements of liquid. Since liquid moves by the least resistant path, it

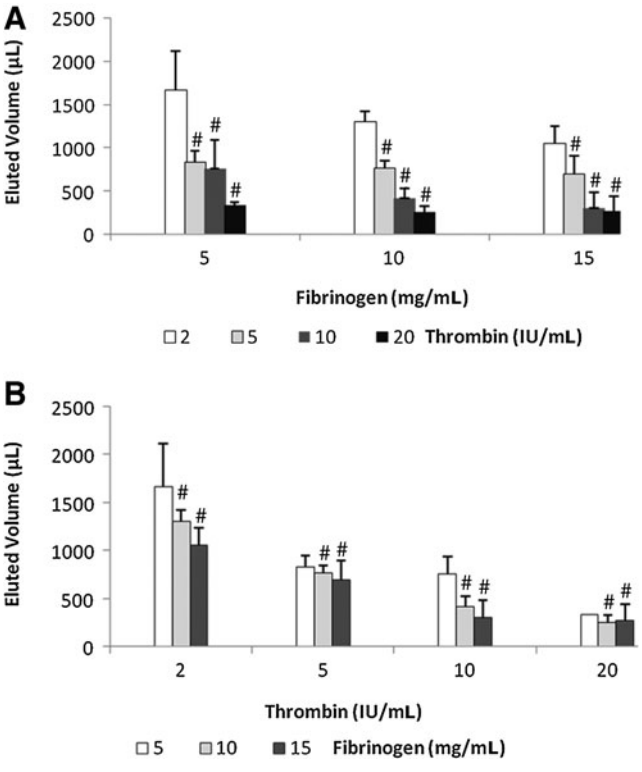

FIG. 2. Flow in 3D fibrin construct depends on fibrinogen and thrombin concentrations. **(A)** Total eluted volume (flow) corresponding to changing fibrinogen concentration at constant thrombin. **(B)** Total eluted volume (flow) corresponding to changing thrombin concentration at constant fibrinogen. 3D, three-dimensional. $^{\#}p < 0.01$.

would suggest that the thrombin and fibrinogen composition does alter the fibrin structure so that movements of liquid mass are greatly affected.

Dependence of the 3D fibrin construct permeability on fibrinogen and thrombin concentration using in vitro *flow assay*

Using the above-established *in vitro* assay, we further examined the permeability in relation to the final fibrinogen and thrombin concentration in a 3D fibrin construct (Fig. 3). Results for the Darcy flow assessment were obtained through modulation of two variables: the hydrostatic pressure head and the fibrinogen concentration used in fibrin formulation. By changing the fibrinogen concentrations with a constant thrombin concentration, porosity change comparisons can be made. Six groups of 3D fibrin constructs were prepared using 8, 10, 12.5, 15, 17.5, and 20 mg/mL fibrinogen solutions to a constant 2 IU/mL thrombin solution. Comparing eluate volume over different hydrostatic pressure settings was used to determine the presence or absence of correlation between pore size and a specific fibrin formulation. The greatest difference in pore size of the same fibrin sample is in the fibrin sample prepared with 8 mg/mL fibrinogen, where the difference is $<2\,\mu$m. Therefore, it is important to take elution measurements over a range of hydrostatic pressure settings to obtain the average radii measurements of fibrin pores.

K_s measurements for the 6 groups of fibrin gels indicate that fibrin samples with greater fibrinogen concentrations yielded slower flow rates for the fibrinogen concentration, that is <12.5 mg/mL. Experimental results evaluated by Student *t*-test analysis showed statistical significance ($^*p<0.05$) of smaller pore radii with increased fibrinogen concentration between 8 mg/mL and all other fibrin samples, where $p<0.0005$ when compared to 20 mg/mL. Additional Student *t*-tests indicated statistical significance ($^{**}p<0.0005$) of a relationship between decreasing pore radii with increasing fibrinogen concentrations between 10 and 20 mg/mL, 12.5 and 20 mg/mL, and 15 and 20 mg/mL. Graphical analysis indicates the inverse relationship between pore radii and fibrinogen concentration for the fibrin samples with lower fibrinogen concentrations (<12.5 mg/mL).

The calculated radius for the fibrin samples with 8 mg/mL fibrinogen is estimated to be $\sim 6.957\,\mu$m. With an increase of fibrinogen concentration from 2 to 10 mg/mL, the radii decreased by ~ 1–$5.881\,\mu$m. An additional 2.5 mg/mL increase of fibrinogen concentration to12.5 mg/mL resulted in the average estimated radius of $\sim 4.928\,\mu$m. Linear regression analysis of the fibrin samples with lower fibrinogen concentrations (≤ 12.5 mg/mL) showed a linear decrease in pore radii with increasing fibrinogen concentrations. R^2 value is evaluated to be >0.99. Bubble showed in Figure 3 shows predicted average pore size (in radius).

In conclusion, there is a corresponding relationship between the permeability and the fibrin composition of fibrinogen and thrombin. As the fibrinogen composition is increased, matrix permeability and average pore size decreased. This trend was also observed in fibrin composition

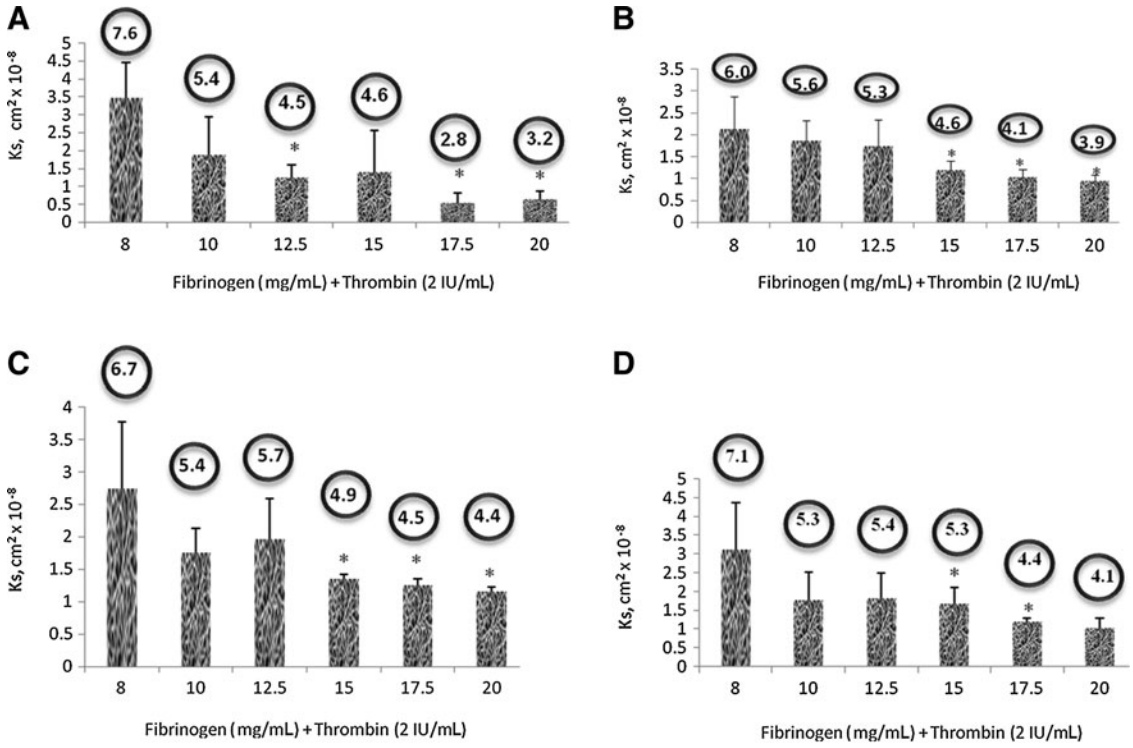

FIG. 3. Plot showing calculated Ks (permeability coefficient) of 3D fibrin constructs of different composition. Bubble shows corresponding predicted average pore size (in radius). Values obtained at different hydrostatic pressure (p-head) corresponding to liquid medium height. Statistical analysis performed using Paired Student *t*-test with significance at $p<0.05$. **(A)** Hydrostatic pressure (p-head) of 160 dyn/cm^2. **(B)** Hydrostatic pressure (p-head) of 460 dyn/cm^2. **(C)** Hydrostatic pressure (p-head) of 750 dyn/cm^2. **(D)** Hydrostatic pressure (p-head) of 890 dyn/cm^2. $^*p<0.05$.

where the thrombin concentration was increased (data not shown). Repeating the experiments at different hydrostatic pressures or flow heights also showed a similar trend. We also observed that as the hydrostatic pressure increased, both the rate of the flow and the standard deviation for our experimental measurements increased. This could be explained by increase in pressure, which causes the deformation of the fibrin matrix and results in the collapse or degradation of the matrix structure, thereby affecting the flow rate.

Diffusion study in a 3D fibrin construct: effect of fibrinogen and thrombin concentration

Dextran molecular probes are used to model possible cell, nutrient, and waste proliferation through 3D fibrin constructs prepared with different fibrinogen concentrations and a constant thrombin concentration of 2 or 5 IU/mL (Fig. 4). Dextran probes in DMEM were added to the 3D fibrin constructs that were seeded on inserts and allowed to diffuse through an 8.0-μm membrane at the bottom of the insert into DMEM. The membrane pores were large enough to allow Dextran particles to diffuse through with minimal obstruction. Dextran particles FITC (3000 MW) and RHO (70,000 MW) were not mixed together in these experiments. After 24 h, aliquots were taken from the bottom of the wells. To ensure uniform sampling of DMEM and Dextran probes, the liquid at the bottom of each well was mixed via pipetting before taking samples for absorbance analysis.

For the Dextran particle FITC, the smaller size probes, there was a steep decrease in diffusion as fibrinogen concentration increased from 5 to 20 mg/mL at both 2 and 5 IU/mL thrombin concentration. The decrease in diffusion was not as steep at fibrinogen concentrations of 10 and 15 mg/mL, when thrombin concentration changes from 2 to 5 IU/mL. This suggests that fibrinogen and thrombin concentration affects the diffusion through small pores in the 3D fibrin constructs.

For the Dextran particle RHO, the large size probes, the effect of fibrinogen and thrombin concentration on diffusion was much less obvious, suggesting that fibrinogen and thrombin concentrations have less effect on the large pores size in 3D fibrin constructs consisting of 5–15 mg/mL of fibrinogen and 2–5 IU/mL of thrombin.

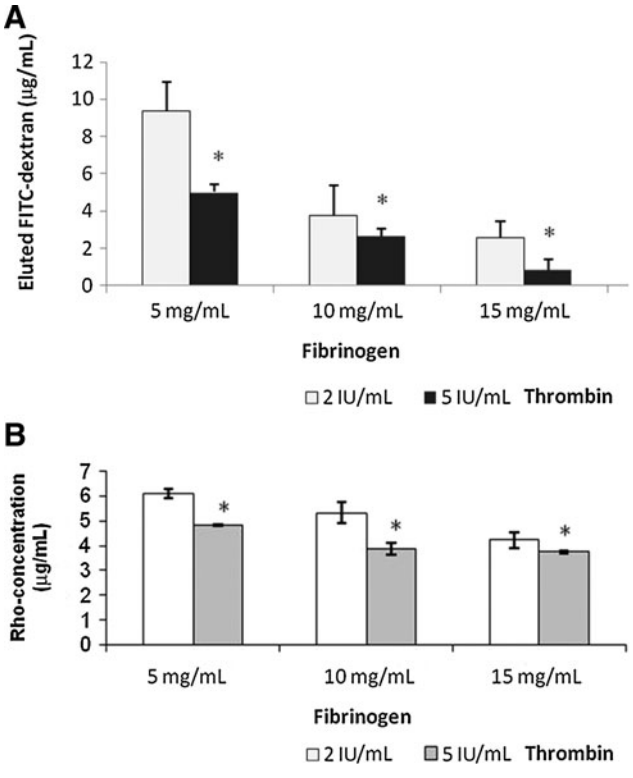

FIG. 4. The effect of fibrin composition on diffusion of FITC-Dextran and Rho-Dextran through fibrin network. **(A)** Diffusion of FITC-Dextran. **(B)** Diffusion of Rho-Dextran. *$p < 0.05$.

Discussion

In this article, we have established that fibrinogen and thrombin concentrations have an inverse relationship with the overall porosity, pore size, and fluid permeability in 3D fibrin constructs. This renders a further relationship between fibrinogen and thrombin concentration to mechanical strength, where similar research has shown that formulations that allow increased crosslinking in 3D fibrin constructs increase the overall mechanical stiffness of fibrin.[6,23] When cells are seeded in 3D fibrin constructs, it is vital that cells are able to migrate, proliferate, and uptake nutrients and gases to reach an optimal tissue growth/regeneration. Because fibrin porosity controls the rate of cellular activity, it is imperative to have controlled 3D fibrin constructs structure for optimal tissue generation.[5]

Although it is illustrated that fibrinogen and thrombin have strong influences over fibrin scaffold ultrastructure, many studies have shown that many other factors also influence the mechanisms of fibrin synthesis.[5] One specific example is the research done by Antovic et al.[24] where acetylsalicylic acid (ASA), an effective antithrombotic agent, when given in low dosage increases fibrin fibril thickness, pore size, and fluid permeability when compared to fibrin without ASA.[24] He et al.[21] analyzed the effects of recombinant factor VIIa (rFVIIa), an enzymatic factor initiating hemostasis in the absence of FVIII and FIX (clotting factors); their analysis showed opposite effects when added to fibrinogen for fibrin synthesis.[21] In FVIII-deficient platelet-containing plasma, increased rFVIIa caused a decrease in porosity, rendering a decrease in fluid permeability when calculated with Darcy's law.[21] Similarly, FIX-deficient platelet-containing plasma also had the same relationship but with weaker magnitudes.[21] Furthermore, Hayen et al.[25] illustrate hyaluronan effects on fibrin fibrils, where fibrin formation in presence of hyaluronan stimulates cell migration by correlation with the fibrin fibrils' mass-to-length ratio. Hence, in achieving specific porosity during fibrin construct synthesis, several factors can be adjusted based on known effective magnitude in changes of each parameter.

In conclusion, a thorough investigation is presented on the effects of porosity and particle diffusivity through various 3D fibrin constructs prepared over a range of fibrin formulations. We showed that fibrinogen content directly affects mass transport and pore dimensions, suggesting that nutrient supply, waste removal, cell migration, and availability of messenger molecules are affected by the final 3D fibrin ultrastructure. The data demonstrate that low concentrations of fibrinogen in 3D constructs support greater diffusion and fluid

flow. Analysis under predicted gradients from mathematical models will be used to fabricate fibrin scaffolds for efficient cell delivery. Next, we are planning to perform environmental scanning electron microscopy to view 3D fibrin constructs, providing visual evidence for changes in fibrin ultrastructure when synthesized under different fibrin formulations.

Disclosure Statement

No competing financial interests exist.

References

1. Sierra D. Fibrin sealant adhesive systems: a review of their chemistry, material properties, and clinical applications. J Biomater Appl. 1993;7:309–352.
2. Albes JM, Klenzner T, Kotzerke J, et al. Improvement of tracheal autograft revascularization by means of fibroblast growth factor. Ann Thorac Surg. 1994;57:444–449.
3. Amrani D. Wound healing: role of commercial fibrin sealants. Ann NY Acad Sci. 2001;936:566–579.
4. Tawil B. Fibrin and Its Applications. Review Article. In: *An Introduction to Biomaterials*. Guelcher SA, Hollinger JO (eds.). Boca Raton, FL: CRC Taylor & Francis; Chapter 7, pp. 105–120; 2005.
5. Duong H, Wu B, Tawil B. Fibrin matrices in tissue engineering. In: *Natural Based Polymers for Biomedical Applications.* Reis RL, Neves NM, Mano JF, et al. (eds.). Cambridge, United Kingdom: Woodhead Publishing Ltd.; 2008.
6. Duong H, Wu B, Tawil B. Modulation of 3-dimensional fibrin matrix stiffness by intrinsic fibrinogen-thrombin compositions and by extrinsic cellular activity. Tissue Eng. 2009;15:1865–1876.
7. Budzynski AZ, Olexa SA. Localization of a fibrin polymerization site. J Biol Chem. 1981;256:3544–3549.
8. Horowitz BH, Varadi A, Scheraga HA. Localization of a fibrin #-chain polymerization site within segment thr-374 to glu-396 of human fibrinogen. Proc Natl Acad Sci USA. 1984;81:5980–5984.
9. Khare A, Woo L, Mclean A, et al. Mechanical characterization of fibrin gels. Blood Coag Fibrinolysis. 1998;9:105.
10. DeMaat MPM, Laurens N, Koolwijk P. Fibrin structure and wound healing. J Thromb Haemost. 2006;4:932.
11. Hall CE, Slayter HS. The fibrinogen molecule: its size, shape and mode of polymerization. J Biophy Biochem Cytol. 1958;5:11–16.
12. Mosesson MW, Siebenlist KR, Meh DA. The structure and biological features of fibrinogen and fibrin. Ann NY Acad Sci. 2001;936:11–30.
13. Ariens RA, Lai T-S, Weisel JW, et al. Role of Factor XIII in fibrin clot formation and effects of genetic polymorphisms. Blood. 2002;100:743–754.
14. Kannan R, Salacinski H, Sales K, et al. The roles of tissue engineering and vascularisation in the development of microvascular networks: a review. Biomaterials. 2005;26:1857–1875.
15. Geckil H, Xu F, Zhang X, et al. Engineering hydrogels as extracellular matrix mimics. Nanomedicine. 2010;5:469–484.
16. Blombäck B, Carlsson K, Fatah K, et al. Fibrin in human plasma: gel architectures governed by rate and nature of fibrinogen activation. Thromb Res. 1994;75:521–538.
17. Soler-Illia GJ, de AA, Sanchez C, et al. Chemical strategies to design textured materials: from microporous and mesoporous oxides to nanonetworks and hierarchical structures. Chem Rev. 2002;102:4093–4138.
18. van Tienen T, Heijkants R, Buma P, et al. Tissue ingrowth and degradation of two biodegradable porous polymers with different porosities and pore sizes. Biomaterials. 2002;23:1731–1738.
19. Wei J, Jia J, Wu F, et al. Hierarchically microporous/macroporous scaffold of magnesium–calcium phosphate for bone tissue regeneration. Biomaterials. 2010;31:1260–1269.
20. Otsuki B, Takemoto M, Fujibayashi S, et al. Pore throat size and connectivity determine bone and tissue ingrowth into porous implants: three-dimensional micro-CT based structural analyses of porous bioactive titanium implants. Biomaterials. 2006;27:5892–5900.
21. He S, Blombäck M, Ekman Jacobsson G, et al. The role of recombinant Factor VIIa (FVIIa) in fibrin structure in the absence of FVIII/FIX. J Thromb Haemost 2003;1:1215–1219.
22. Okada M, Blombäck B. Factors influencing fibrin gel structure studied by flow measurement. Ann NY Acad Sci. 2006;408:233–253.
23. Standeven KF, Carter AM, Grant PJ, et al. Functional analysis of fibrin γ-chain cross-linking by activated Factor XIII: determination of a cross-linking pattern that maximizes clot stiffness. Blood. 2007;110:902–907.
24. Antovic A, Perneby C, Ekman GJ, et al. Marked increase of fibrin gel permeability with very low dose ASA treatment. Thromb Res. 2005;116:509–517.
25. Hayen W, Goebeler M, Kumar S, et al. Hyaluronan stimulates tumor cell migration by modulating the fibrin fiber architecture. J Cell Sci. 1999;112:2241–2251.

Address correspondence to:
Bill Tawil, PhD, MBA
Department of Bioengineering
University of California
420 Westwood Plaza
Room 5121, Engineering V.
P.O. Box 951600
Los Angeles, CA 90095-1600

E-mail: btawil@seas.ucla.edu